An Accurate Virtual Signal Injection Control for IPMSM With Improved Torque Output and Widen Speed Region

Zhiwei Chen, Yan Yan, Tingna Shi, *Member, IEEE*, Xin Gu, *Member, IEEE*, Zhiqiang Wang, *Member, IEEE*, and Changliang Xia, *Senior Member, IEEE*

***Abstract*—A method of current reference setting for interior permanent magnet synchronous motor based on virtual constant signal injection is proposed. Unlike traditional methods, the partial derivative of torque to d-aixs, q-axis currents is obtained by injecting a virtual constant signal into d-axis, q-axis currents, then the derivative of torque to current angle is obtained through the full differential equation. A scheme of current reference setting, which is applicable to constant torque region and flux-weakening region, is established by means of the derivative information. The difference between the voltage output by the current controller and the actual voltage applied to the motor is also analyzed. Filters that are essential in the virtual sinusoidal signal injection scheme are avoided. Moreover, the acquisition of partial derivative information avoids the influence of neglecting high-order partial derivative term from which the method of injecting virtual square wave signal along the current angle suffers. This method not only realizes maximum torque per ampere control, accurately, but also guarantees the speed range of constant torque region by the setting of q-axis current reference, which is parameter independent. Meanwhile, the torque output capacity is assured in the flux-weakening region. Finally, the proposed method is verified by experiments.**

***Index Terms*—Flux-weakening (FW) control, interior permanent magnet synchronous motor (IPMSM), maximum torque per ampere (MTPA), virtual signal injection.**

Manuscript received January 14, 2020; revised April 29, 2020 and June 12, 2020; accepted July 14, 2020. Date of publication July 20, 2020; date of current version September 22, 2020. This work was supported in part by the Major Program of National Natural Science Foundation of China under Grant 51690183, in part by the Fundamental Research Funds for the Central Universities under Grant 2020QNA4012, and in part by the Natural Science Foundation of Tianjin under Grant 19JCYBJC21800. Recommended by Associate Editor B. Mirafzal. *(Corresponding authors: Yan Yan; Tingna Shi.)*

Zhiwei Chen is with the School of Electrical and Information Engineering, Tianjin University, Tianjin 300072, China (e-mail: chenzw@tju.edu.cn).

Yan Yan and Tingna Shi are with the Zhejiang Provincial Key Laboratory of Electrical Machine Systems, College of Electrical Engineering, Zhejiang University, Hangzhou 310027, China (e-mail: yan_yan@zju.edu.cn; tnshi@zju.edu.cn).

Xin Gu and Zhiqiang Wang are with the School of Electrical Engineering and Automation, Tiangong University, Tianjin 300387, China (e-mail: guxin@tiangong.edu.cn; wangzhq@tju.edu.cn).

Changliang Xia is with the School of Electrical Engineering and Automation, Tiangong University, Tianjin 300387, China, and also with the Zhejiang Provincial Key Laboratory of Electrical Machine Systems, College of Electrical Engineering, Zhejiang University, Hangzhou 310027, China (e-mail: motor@tju.edu.cn).

Color versions of one or more of the figures in this article are available online at https://ieeexplore.ieee.org.

Digital Object Identifier 10.1109/TPEL.2020.3010300

I. Introduction

INTERIOR permanent magnet synchronous motor (IPMSM) is widely used in the electric vehicle drive system because of the advantages of compact structure, high power density, and wide flux-weakening (FW) range [1]. However, the uncertainty of the parameters due to magnetic saturation and cross-coupling effects trigger its control far from excellent [2].

Normally, maximum torque per ampere (MTPA) control is often used in constant torque region. With the speed increasing, FW control is used in order to meet the constraints of the current and voltage limits [3]. Due to the fact that torque control is the control mode of the electric vehicle drive system, how to reasonably arrange the d-axis and q-axis current references under torque control mode has become a key factor affecting the performance of the motor.

At first, the MTPA points are calculated with constant parameters [2]–[4]. However, the control performance of these methods is seriously affected by parameters in real industrial applications. In order to solve this problem, various methods have been presented. The method of MTPA published in literature can be classified into two categories.

One is the offline method that often employs lookup table (LUT) to facilitate the MTPA control [5]–[7]. With LUTs, the motor parameters or current references can be obtained with the searching index of d–q currents combination or torque–flux one, respectively. To some degree, the way of LUT reduces the influence caused by the change of the motor parameters on current references. However, In order to consider the ambient temperature and the operation condition of the motor, a large number of experiments need to be carried out in advance, which is obviously tedious. And, it is not practical to perform tests on each individual machine. Meanwhile, linear interpolation calculation, which has some errors, often used to obtain the references. These factors greatly restrict the application scope of these methods.

The other is the online method that attracts the attention of scholars due to its portability. These methods can be further classified as online parameter estimation methods [8], model-based method [9]–[13], and signal injection methods [14]–[27]. The online parameter estimation methods use the identification method to realize the online motor parameter estimation and then realize the MTPA control of the motor. For example,

the recursive least square method is used to estimate q-axis inductance and permanent flux linkage, and then the MTPA control is realized by combining adaptive control in [8]. In general, model-based method is establishing a mathematical model with constant motor parameters, thus realizing the MTPA point search by combining intelligent control algorithm or control law, such as recurrent Legendre fuzzy neural network [9], variable-equivalent-parameter MTPA control law [10], and parameters self-modification [11]. Although these methods can realize MTPA control, they are usually complex to implement.

The signal injection method is an alternative to online methods that can be divided into real signal injection method and virtual signal injection method. The real signal injection method is injecting a periodic signal, which can be sinusoidal, square wave, or step signal, into the current, flux reference, or voltage vector in the control loop [14]–[19]. Thus, the current angle (β) can be adjusted. Finally, the MTPA control can be realized by using the condition that the derivative of the torque to the current angle is zero. These methods can achieve accurate acquisition of MTPA points, but additional signal injection leads to additional copper loss, inevitably.

In recent years, some scholars proposed MTPA control methods with virtual signal injection [20]–[27]. At first, a virtual sinusoidal signal is injected into the calculated β and extract the derivative of torque with respect to β to realize the MTPA control [20]–[25]. Because the sinusoidal signal is not injected into the motor control loop actually, the extra loss is avoided. However, the speed of the d-axis current reference setting is quite slow due to the use of overmuch filters. In order to solve this problem, the virtual square wave signal injection method is proposed [26], [27]. A square signal injected along the current angle removes the utilization of filters. However, the derivative information obtained will be affected by the high-order partial derivative term which is neglected. In order to make full use of the IPMSM, it not only realizes MTPA control of the motor but also should arrange the q-axis current reference, reasonably. The setting of q-axis current reference which is parameter independent is the key to ensure the motor torque output capacity. It is not suitable that the q-axis current reference is calculated with constant parameters in [20]–[23].

As the speed increases, MTPA control cannot meet the constraints of the current and voltage limits. So, how to set the d-axis and q-axis current references is needed in FW region. The common solutions are feedforward methods, feedback methods, and mixed methods. The feedforward methods use LUTs to determine the current references [5]–[7]. The feedback methods take the error between the motor terminal voltage and voltage limit as the feedback information and then generate the correction amount of d-axis current reference through the PI controller [28]–[30]. Although the above feedback methods can be used in the speed control mode independently of the motor parameters, it is still difficult to reasonably arrange the q-axis current reference in the torque control mode. The mixed methods combine the feedforward methods with the feedback methods [31]–[33]. In order to determine the current references in full speed region, a method of virtual sinusoidal signal injection combined with feedback methods is proposed [23]. However, the control performance of this method is affected by the mode of setting of q-axis current reference which is calculated by the formula with constant parameters.

For IPMSM often used in vehicle applications, how to determine the currents references in MTPA and flux weakening region is a very meaningful and challenging work [23]. Based on this background, this article proposes a strategy to determine the d-axis and q-axis current references based on virtual constant signal injection. Unlike the traditional injection of virtual sinusoidal or square wave signals along the current angle, a constant signal is superimposed on the d-axis and q-axis currents to obtain the partial derivative information of torque with respect to the d-axis and q-axis current, respectively, and then the $\mathrm{d}T_\mathrm{e}/\mathrm{d}\beta$ is obtained through the full differential equation. A scheme of d-axis and q-axis current references setting, which is applicable to constant torque region and FW region, is established by means of the derivative of torque to current angle and the partial derivative of torque to q-axis current. At the same time, the difference between the voltage output by the current controller and the actual voltage applied to the motor caused by the rotor movement during one control period is analyzed. By the voltage correction, the applied voltage to the motor is restored, which improves the accuracy of extracting partial derivative information. This method not only realizes accurate MTPA control but also guarantees the speed range of constant torque region by setting of q-axis current reference which is parameter independent. Meanwhile, the torque output capacity is assured in FW region.

II. System Model and Steady-State Operating Point

A. IPMSM d–q Model

In the synchronous frame, the voltage and torque equation of an IPMSM can be expressed as [4]

$$\begin{bmatrix} v_\mathrm{d} \\ v_\mathrm{q} \end{bmatrix} = \begin{bmatrix} R+\mathrm{p}L_\mathrm{d} & -\omega_\mathrm{e}L_\mathrm{q} \\ \omega_\mathrm{e}L_\mathrm{d} & R+\mathrm{p}L_\mathrm{q} \end{bmatrix} \begin{bmatrix} i_\mathrm{d} \\ i_\mathrm{q} \end{bmatrix} + \begin{bmatrix} 0 \\ \omega_\mathrm{e}\lambda_\mathrm{f} \end{bmatrix} \tag{1}$$

$$T_\mathrm{e} = \frac{3}{2} n_\mathrm{p}[\lambda_\mathrm{f} i_\mathrm{q} + (L_\mathrm{d} - L_\mathrm{q}) i_\mathrm{q} i_\mathrm{d}]. \tag{2}$$

In steady–state operation, the voltage equation can be expressed as [4]

$$\begin{cases} v_\mathrm{d} = Ri_\mathrm{d} - \omega_\mathrm{e}L_\mathrm{q}i_\mathrm{q} \\ v_\mathrm{q} = Ri_\mathrm{q} + \omega_\mathrm{e}L_\mathrm{d}i_\mathrm{d} + \omega_\mathrm{e}\lambda_\mathrm{f} \end{cases} \tag{3}$$

where v_d and v_q are the stator voltage components of the motor in d–q frame; R is the stator resistance; i_d and i_q are the currents in d–q frame; L_d and L_q represent the d-axis stator inductance and q-axis stator inductance, respectively; λ_f and ω_e are the stator flux linkage of the permanent magnet and electrical angular velocity, respectively; p is the differential symbol; and n_p represents the number of pole pairs.

B. Voltage and Current Limit and Steady-State Operating Point

1) Equation of current limit is [3]*:*

$$\left(i_\mathrm{d}^2 + i_\mathrm{q}^2\right) \le I_\mathrm{lim}^2 \tag{4}$$

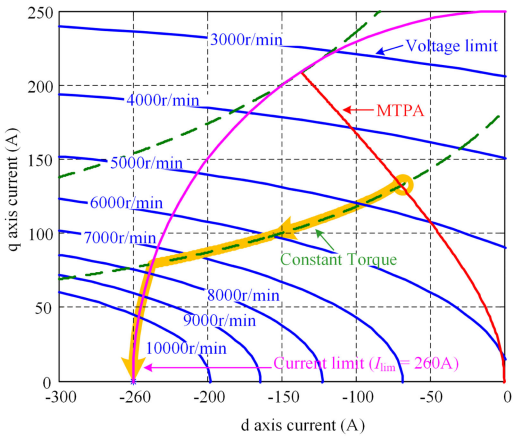

Fig. 1. IPMSM current track with a given torque in the full speed domain.

where $I_{\lim}$ is the maximum allowable current of the motor system, which is determined by the current level of the system and the heat dissipation capacity. Considering a long time running of the motor, the current limit is generally set as the rated current.

2) Equation of voltage limit is [3]*:*

$$\left(v_{\mathrm{d}}^2+v_{\mathrm{q}}^2\right)\le V_{\lim}^2 \tag{5}$$

where $V_{\lim}$ is the maximum available inverter output fundamental voltage, which is determined by dc-side voltage of the inverter and modulation strategy. Assuming that stator resistance can be ignored and combined with (1), (5) can be rewritten as [3]

$$\left(L_{\mathrm{d}}i_{\mathrm{d}}+\lambda_{\mathrm{f}}\right)^2+\left(L_{\mathrm{q}}i_{\mathrm{q}}\right)^2\le\left(\frac{V_{\lim}}{\omega_{\mathrm{e}}}\right)^2. \tag{6}$$

As shown in (6), voltage limit is an ellipse in d–q axis current frame.

3) MTPA Control: The torque of IPMSM composes two parts, i.e., excitation torque and reluctance torque, and its expression is [11]

$$T_{\mathrm{e}}=\frac{3}{2}n_{\mathrm{p}}\left[\lambda_{\mathrm{f}}I_{\mathrm{s}}\cos\beta-\frac{1}{2}\left(L_{\mathrm{d}}-L_{\mathrm{q}}\right)I_{\mathrm{s}}^2\sin 2\beta\right] \tag{7}$$

where I_{s} is the amplitude of the current vector; β is the angle between the current vector and the q axis. When the amplitude of the current vector is constant, there is an optimal current angle to maximize the output torque of the IPMSM. And it can be expressed as follows [20]:

$$\beta=\sin^{-1}\left(\frac{-\lambda_{\mathrm{f}}+\sqrt{\lambda_{\mathrm{f}}^2+8\left(L_{\mathrm{q}}-L_{\mathrm{d}}\right)^2I_{\mathrm{s}}^2}}{4\left(L_{\mathrm{q}}-L_{\mathrm{d}}\right)I_{\mathrm{s}}}\right). \tag{8}$$

MTPA control can be achieved by setting the d-axis current reference in this current angle. $\mathrm{d}T_{\mathrm{e}}/\mathrm{d}\beta$ equals zero is the characteristic of MTPA control.

4) Steady-State Operating Point: The steady-state operating point of the motor is determined by the motor speed, torque, voltage, current limit, and other factors. As shown in Fig. 1, for a given torque, the current references of IPMSM in the full speed region can be determined according to the following rules:

1) when the motor terminal voltage and current do not reach the limit, the d-axis and q-axis current references are determined by MTPA control;
2) as the speed increases, the output voltage of the inverter reaches the limit. At this point, the d-axis and q-axis current references should be the intersection point of the constant torque curve and voltage limit ellipse;
3) as the speed continues to increase, the d-axis and q-axis current references should be the intersection of the current limit circle and the voltage limit ellipse, which are constrained by the current limit.

III. Error Analysis of Traditional Virtual Signal Injection Method

The MTPA control method based on virtual signal injection is to virtually superimpose a periodic signal on the detected current angle (β), then the $\mathrm{d}T_{\mathrm{e}}/\mathrm{d}\beta$ information is obtained to realize the MTPA control. Initially, a sinusoidal signal is injected into the current angle. The $\mathrm{d}T_{\mathrm{e}}/\mathrm{d}\beta$ information is obtained through low-pass and band-pass filters, and then it is used as a feedback signal to adjust the d-axis current reference. However, the uncertainty of the motor parameters could affect the setting of q-axis current reference in torque control mode which is calculated by the formula in this method.

In order to reduce the use of filters, a square wave signal of the following form is injected into the current angle [26], [27]:

$$r\left(t\right)=\begin{cases}0, NT_{\mathrm{h}}\le t<\left(N+0.5\right)T_{\mathrm{h}}\\ \rho, \left(N+0.5\right)T_{\mathrm{h}}\le t<\left(N+1\right)T_{\mathrm{h}}\end{cases} \tag{9}$$

where N is a positive integer; T_{h} is the period of the signal. $r(t)$ is added into β and substituted for β in (7)

$$T_{\mathrm{e}}^{\mathrm{h}}=\frac{3}{2}n_{\mathrm{p}}\left[\lambda_{\mathrm{f}}I_{\mathrm{s}}\cos(\beta+r)-\frac{1}{2}\left(L_{\mathrm{d}}-L_{\mathrm{q}}\right)I_{\mathrm{s}}^2\sin 2(\beta+r)\right] \tag{10}$$

when $(N+0.5)T_{\mathrm{s}}\le t<(N+1)T_{\mathrm{s}}$, the torque after adding periodic signal is expanded by Taylor's series at the point $(i_{\mathrm{d}}, i_{\mathrm{q}})$ [23]

$$T_{\mathrm{e}}^{\mathrm{h}}=T_{\mathrm{e}}(\beta)+\rho\left(\frac{\partial T_{\mathrm{e}}}{\partial\beta}+\underbrace{\frac{1}{2}\rho\frac{\partial^2T_{\mathrm{e}}}{\partial\beta^2}+\frac{1}{6}\rho^2\frac{\partial^3T_{\mathrm{e}}}{\partial\beta^3}\cdots}_{\Delta}\right). \tag{11}$$

The virtual square wave signal injection method ignores the higher order partial derivative term in (11), thus obtaining information directly. However, since torque is a trigonometric function of the current angle, ignoring its higher order partial derivatives may affect the accuracy of the extracted information to some extent. According to (10) and (11), the difference between the extracted partial derivative and the actual partial derivative (Δ) can be expressed as the function of β, I_{s}, and ρ

$$\Delta=f(I_{\mathrm{s}},\beta,\rho),\beta\in(0,\pi/2). \tag{12}$$

According to (12), Fig. 2 shows the relation between the error of partial derivative information, the amplitude of the current (I_{s}) and current angle (β). In the figure, The amplitude of the injected square wave signal is 0.1 and 0.2, respectively. It can be seen that the error of partial derivative increases with the amplitude of

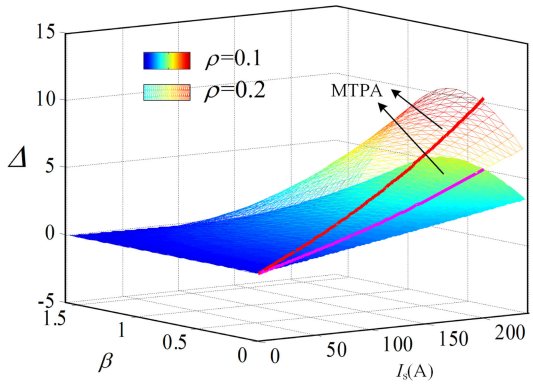

Fig. 2. Error of extracted partial derivative at different current amplitudes, current angle, and amplitude of the injected signal.

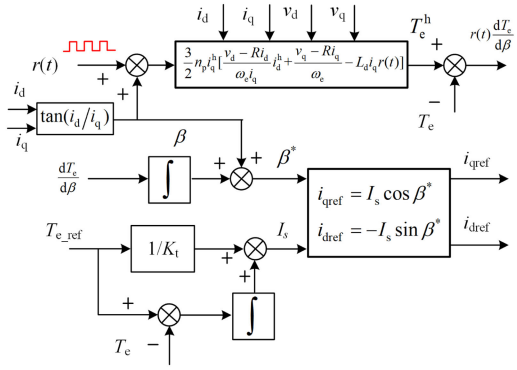

Fig. 3. Logic of d-axis and q-axis current generation of the virtual square signal injection method.

current and injected signal. As the current amplitude is constant, the error increases with the increase of the current angle at first and then decreases. Therefore, the traditional virtual square wave signal injection method is difficult to obtain accurate partial derivative information.

In order to reduce the influence of motor parameters on the setting of q-axis current reference, the difference between the torque calculated by the torque formula and the reference is used to generate the correction of the given current amplitude I_s through a PI controller, and then the q-axis reference is generated by using current angle. The scheme of this method is given in Fig. 3.

The above analysis is carried out without considering the voltage error. In fact, the influence of the dead-time of the inverter, the delay of the control cycle, and other factors can also lead to the difference between the voltage output by the current controller and the actual voltage applied to the motor, which will also affect the accuracy of the derivative of torque with respect to β.

IV. Proposed Method of Currents Setting Based on Virtual Constant Signal Injection

In order to improve the accuracy of the derivative of torque with respect to β and achieve the purpose of the q-axis current reference setting which is parameter independent, a scheme of d-axis and q-axis current references setting, which is based on a virtual constant signal injection, is proposed.

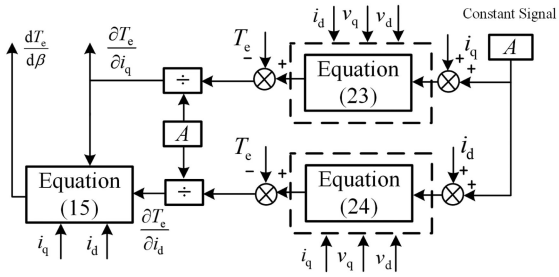

Fig. 4. Schematic of proposed virtual constant signal injecton.

A. Principle of Obtaining $dT_e/d\beta$

The relationships between d-axis and q-axis current and current angle (β) are as follow:

$$\begin{cases} i_{\mathrm{q}} = I_{\mathrm{s}} \cos\beta \\ i_{\mathrm{d}} = -I_{\mathrm{s}} \sin\beta. \end{cases} \tag{13}$$

The total differential equation can be represented as

$$\frac{\mathrm{d}T_{\mathrm{e}}}{\mathrm{d}\beta} = \frac{\partial T_{\mathrm{e}}}{\partial i_{\mathrm{d}}}\frac{\mathrm{d}i_{\mathrm{d}}}{\mathrm{d}\beta} + \frac{\partial T_{\mathrm{e}}}{\partial i_{\mathrm{q}}}\frac{\mathrm{d}i_{\mathrm{q}}}{\mathrm{d}\beta}. \tag{14}$$

From (13) and (14), $\mathrm{d}T_{\mathrm{e}}/\mathrm{d}\beta$ can be obtained

$$\begin{aligned} \frac{\mathrm{d}T_{\mathrm{e}}}{\mathrm{d}\beta} &= \frac{\partial T_{\mathrm{e}}}{\partial i_{\mathrm{d}}}\left(-I_{\mathrm{s}}\cos\beta\right) + \frac{\partial T_{\mathrm{e}}}{\partial i_{\mathrm{q}}}\left(-I_{\mathrm{s}}\sin\beta\right) \\ &= -\frac{\partial T_{\mathrm{e}}}{\partial i_{\mathrm{d}}} i_{\mathrm{q}} + \frac{\partial T_{\mathrm{e}}}{\partial i_{\mathrm{q}}} i_{\mathrm{d}}. \end{aligned} \tag{15}$$

In order to obtain $\mathrm{d}T_{\mathrm{e}}/\mathrm{d}\beta$, the partial derivatives of torque to d-axis and q-axis currents need to be obtained, first. A method is presented to extract two partial derivatives by injecting a constant signal into the detected d-axis and q-axis currents, respectively. The control block is shown in Fig. 4.

According to (2), the torque after injecting the constant signal A is expressed as

$$\begin{cases} T_{\mathrm{e}}^{\mathrm{h}}(i_{\mathrm{d}}, i_{\mathrm{q}} + A) = \frac{3}{2} n_{\mathrm{p}} \left[\left(L_{\mathrm{d}} - L_{\mathrm{q}}\right) i_{\mathrm{d}} + \lambda_{\mathrm{f}}\right] \left(i_{\mathrm{q}} + A\right) \\ T_{\mathrm{e}}^{\mathrm{h}}(i_{\mathrm{d}} + A, i_{\mathrm{q}}) = \frac{3}{2} n_{\mathrm{p}} \left[\left(L_{\mathrm{d}} - L_{\mathrm{q}}\right) \left(i_{\mathrm{d}} + A\right) + \lambda_{\mathrm{f}}\right] i_{\mathrm{q}}. \end{cases} \tag{16}$$

Taking $T_{\mathrm{e}}^{\mathrm{h}}(i_{\mathrm{d}}, i_{\mathrm{q}} + A)$ as an example, binary Taylor's series expansion can be carried out at the point $(i_{\mathrm{d}}, i_{\mathrm{q}})$

$$T_{\mathrm{e}}^{\mathrm{h}}(i_{\mathrm{d}}, i_{\mathrm{q}} + A) = T_{\mathrm{e}}(i_{\mathrm{d}}, i_{\mathrm{q}}) + A\frac{\partial T_{\mathrm{e}}}{\partial i_{\mathrm{q}}} + \frac{1}{2}A^2 \frac{\partial}{\partial i_{\mathrm{q}}}\left(\frac{\partial T_{\mathrm{e}}}{\partial i_{\mathrm{q}}}\right) + \cdots. \tag{17}$$

Since there is no i_{q} term in $\partial T_{\mathrm{e}}/\partial i_{\mathrm{q}}$, the second and above partial derivatives are all zero, so (17) is equivalent to

$$T_{\mathrm{e}}^{\mathrm{h}}(i_{\mathrm{d}}, i_{\mathrm{q}} + A) = T_{\mathrm{e}} + A\frac{\partial T_{\mathrm{e}}}{\partial i_{\mathrm{q}}}. \tag{18}$$

So $\partial T_{\mathrm{e}}/\partial i_{\mathrm{q}}$ can be expressed as

$$\frac{\partial T_{\mathrm{e}}}{\partial i_{\mathrm{q}}} = \left[T_{\mathrm{e}}^{\mathrm{h}}(i_{\mathrm{d}}, i_{\mathrm{q}} + A) - T_{\mathrm{e}}\right]/A. \tag{19}$$

Similarly

$$\frac{\partial T_{\mathrm{e}}}{\partial i_{\mathrm{d}}} = \left[T_{\mathrm{e}}^{\mathrm{h}}(i_{\mathrm{d}}+A, i_{\mathrm{q}}) - T_{\mathrm{e}}\right]/A. \tag{20}$$

When the motor parameters are known, the required partial derivative can be obtained by substituting (2) and (16) into (19) and (20). In order to avoid the influence of parameter changes on obtaining partial derivative, the following transformation is required [23]. It can be derived from (3) that

$$L_{\mathrm{q}} = -\frac{v_{\mathrm{d}} - Ri_{\mathrm{d}}}{\omega_{\mathrm{e}} i_{\mathrm{q}}}, L_{\mathrm{d}} i_{\mathrm{d}} + \lambda_{\mathrm{f}} = \frac{v_{\mathrm{q}} - Ri_{\mathrm{q}}}{\omega_{\mathrm{e}}}. \tag{21}$$

Substituting (21) into (2) and (16)

$$T_{\mathrm{e}}(i_{\mathrm{d}}, i_{\mathrm{q}}) = \frac{3}{2} n_{\mathrm{p}} \left[\frac{v_{\mathrm{q}} - Ri_{\mathrm{q}}}{\omega_{\mathrm{e}}} + \frac{v_{\mathrm{d}} - Ri_{\mathrm{d}}}{\omega_{\mathrm{e}} i_{\mathrm{q}}} i_{\mathrm{d}}\right] i_{\mathrm{q}} \tag{22}$$

$$T_{\mathrm{e}}^{\mathrm{h}}(i_{\mathrm{d}}, i_{\mathrm{q}}+A) = \frac{3}{2} n_{\mathrm{p}} \left[\frac{v_{\mathrm{q}} - Ri_{\mathrm{q}}}{\omega_{\mathrm{e}}} + \frac{v_{\mathrm{d}} - Ri_{\mathrm{d}}}{\omega_{\mathrm{e}} i_{\mathrm{q}}} i_{\mathrm{d}}\right] (i_{\mathrm{q}}+A) \tag{23}$$

$$T_{\mathrm{e}}^{\mathrm{h}}(i_{\mathrm{d}}+A, i_{\mathrm{q}}) = \frac{3}{2} n_{\mathrm{p}} i_{\mathrm{q}} \left[\frac{v_{\mathrm{q}} - Ri_{\mathrm{q}}}{\omega_{\mathrm{e}}} + L_{\mathrm{d}} A + \frac{v_{\mathrm{d}} - Ri_{\mathrm{d}}}{\omega_{\mathrm{e}} i_{\mathrm{q}}} (i_{\mathrm{d}}+A)\right]. \tag{24}$$

Compared with the traditional virtual square wave signal injection method, this method indirectly obtains $\mathrm{d}T_{\mathrm{e}}/\mathrm{d}\beta$ which avoids the influence of ignoring the higher order partial derivatives and does not use filters.

B. Influence of Voltage Error on Partial Derivative Information Extraction and Voltage Correction

There is no d-axis, q-axis inductance, and stator flux linkage of the permanent magnet in (22) and (23). So, the partial derivative of the torque to the q-axis current is not affected by the motor parameters. Although the d-axis inductance is included in (24), the change of d-axis inductance is relatively small compared with the change of q-axis inductance in the MTPA control range. So, the effect of q-axis inductance is more prominent than d-axis inductance [26]. And, although stator resistance is used, it is small for IPMSM which is often used in vehicle applications. So, the influence of stator resistance can be ignored [20].

The accuracy of the partial derivative information obtained depends on the accuracy of the d-axis and q-axis currents, d-axis and q-axis voltages, and rotational speed. Among them, it is difficult to accurately obtain d-axis and q-axis voltages, due to the influence of the inverter nonlinearity and other factors. The influence of voltage error on the extraction of torque information is analyzed as follows.

Taking (24) as an example, L_{d0} substituted for L_{d}

$$T_{\mathrm{e0}}^{\mathrm{h}}(i_{\mathrm{d}}+A, i_{\mathrm{q}}) = \frac{3}{2} n_{\mathrm{p}} i_{\mathrm{q}} \left[\frac{v_{\mathrm{q0}} - Ri_{\mathrm{q}}}{\omega_{\mathrm{e}}} + L_{\mathrm{d0}} A + \frac{v_{\mathrm{d0}} - Ri_{\mathrm{d}}}{\omega_{\mathrm{e}} i_{\mathrm{q}}} (i_{\mathrm{d}}+A)\right] \tag{25}$$

where v_{d0} and v_{q0} are, respectively, the d-axis and q-axis voltages which current controller output, and L_{d0} is the nominal value of the d-axis inductance. With the influence of the inverter nonlinearity, the relation between the output voltage of the current controller and the actual voltage applied to the motor can be represented as

$$\begin{cases} v_{\mathrm{q}} = v_{\mathrm{q0}} - \Delta v_{\mathrm{q}} \\ v_{\mathrm{d}} = v_{\mathrm{d0}} - \Delta v_{\mathrm{d}} \end{cases} \tag{26}$$

where Δv_{d} and Δv_{q} are, respectively, the errors of d-axis and q-axis voltages.

According to (24)–(26), the error can be obtained as

$$\Delta T_{\mathrm{e}}^{\mathrm{h}}(i_{\mathrm{d}}+A, i_{\mathrm{q}}) = \frac{3}{2} n_{\mathrm{p}} i_{\mathrm{q}} \left[\frac{\Delta v_{\mathrm{q}}}{\omega_{\mathrm{e}}} + (L_{\mathrm{d0}} - L_{\mathrm{d}})A + \frac{\Delta v_{\mathrm{d}}}{\omega_{\mathrm{e}} i_{\mathrm{q}}} (i_{\mathrm{d}}+A)\right]. \tag{27}$$

Similarly

$$\Delta T_{\mathrm{e}}^{\mathrm{h}}(i_{\mathrm{d}}, i_{\mathrm{q}}+A) = \frac{3}{2} n_{\mathrm{p}} \left(\frac{\Delta v_{\mathrm{q}}}{\omega_{\mathrm{e}}} + \frac{\Delta v_{\mathrm{d}}}{\omega_{\mathrm{e}} i_{\mathrm{q}}} i_{\mathrm{d}}\right) (i_{\mathrm{q}}+A) \tag{28}$$

$$\Delta T_{\mathrm{e}}(i_{\mathrm{d}}, i_{\mathrm{q}}) = \frac{3}{2} n_{\mathrm{p}} \left(\frac{\Delta v_{\mathrm{q}}}{\omega_{\mathrm{e}}} + \frac{\Delta v_{\mathrm{d}}}{\omega_{\mathrm{e}} i_{\mathrm{q}}} i_{\mathrm{d}}\right) i_{\mathrm{q}}. \tag{29}$$

Further, the partial derivative error caused by voltage error can be expressed as

$$\begin{cases} \Delta\left(\frac{\partial T_{\mathrm{e}}}{\partial i_{\mathrm{q}}}\right) = \frac{3}{2} n_{\mathrm{p}} \left(\frac{\Delta v_{\mathrm{q}}}{\omega_{\mathrm{e}}} + \frac{\Delta v_{\mathrm{d}}}{\omega_{\mathrm{e}} i_{\mathrm{q}}} i_{\mathrm{d}}\right) \\ \Delta\left(\frac{\partial T_{\mathrm{e}}}{\partial i_{\mathrm{d}}}\right) = \frac{3}{2} n_{\mathrm{p}} i_{\mathrm{q}} \left[(L_{\mathrm{d0}} - L_{\mathrm{d}}) + \frac{\Delta v_{\mathrm{d}}}{\omega_{\mathrm{e}} i_{\mathrm{q}}}\right] \\ \Delta\left(\frac{\partial T_{\mathrm{e}}}{\partial \beta}\right) = \frac{3}{2} n_{\mathrm{p}} \left[\frac{\Delta v_{\mathrm{d}}}{\omega_{\mathrm{e}} i_{\mathrm{q}}} \left(i_{\mathrm{d}}^2 - i_{\mathrm{q}}^2\right) + \frac{\Delta v_{\mathrm{q}}}{\omega_{\mathrm{e}}} i_{\mathrm{d}} - (L_{\mathrm{d0}} - L_{\mathrm{d}})\, i_{\mathrm{q}}^2\right]. \end{cases} \tag{30}$$

It can be seen that the voltage errors of d-axis and q-axis voltages will affect the accuracy of the extracted partial derivative information.

In practical application, the most direct way is that the voltage output by the current controller is used as the voltage applied to the motor [20]–[22]. However, due to the fact that the dead-time of the inverter can cause a difference between the actual motor terminal voltage and the voltage output by the current controller, the output of voltages by the current controller with dead-time compensation is used by some scholars [26], [27]. The dc-bus voltage detected by the sensor and the duty cycle calculated, which include dead-time, is used to obtain the voltages by [16]. Moreover, it can be found that the rotor position change caused by the delay of the control cycle is another important reason for this difference, especially at high speed. There is no reasonable consideration and analysis of this error in the existing method.

In the vector control system, the typical time sequence of current sampling, computation, and PWM output is shown in Fig. 5(a). Due to the digital controller, the current controller output voltage vector ($\boldsymbol{V}$) obtained at the time of (0) can only function at the beginning of the next control cycle (T_{s}), during which the position of the motor rotor changes by $\omega_{\mathrm{e}} T_{\mathrm{s}}$. The rotor position of the motor continues to change during the control cycle where $\boldsymbol{V}$ acts. The rotor position of the motor changes by $\omega_{\mathrm{e}} T_{\mathrm{s}}$ at the end of the control cycle ($2T_{\mathrm{s}}$). The schematic diagram of the d-axis and q-axis voltage changes caused by rotor position changes is shown in Fig. 5(b).

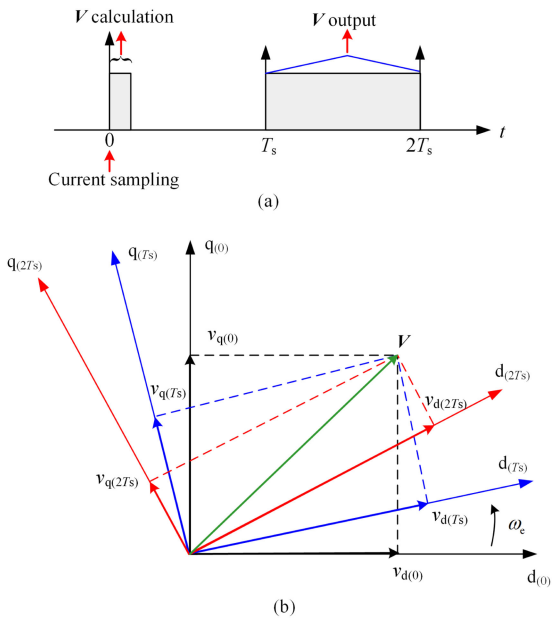

Fig. 5. Diagram of the output voltage of current controller and actual motor terminal voltage. (a) Time sequence of current sampling, calculation, and voltage output. (b) Diagram of d–q axis voltage change caused by rotor position change.

Assuming that $\boldsymbol{V}$ at the time of (0) is expressed as $\boldsymbol{v}_{\mathrm{dq}(0)}$ in the coordinate of $\mathrm{d}_{(0)}\mathrm{q}_{(0)}$. At the time of ($T_\mathrm{s}$), $\boldsymbol{V}$ is expressed as $\boldsymbol{v}_{\mathrm{dq}(\,T\mathrm{s})}$ in the coordinate of $\mathrm{d}_{(\,T\mathrm{s})}\mathrm{q}_{(\,T\mathrm{s})}$. There is a relation between $\boldsymbol{v}_{\mathrm{dq}(0)}$ and $\boldsymbol{v}_{\mathrm{dq}(\,T\mathrm{s})}$

$$\boldsymbol{v}_{\mathrm{dq}(T_\mathrm{s})} = \mathrm{e}^{-\mathrm{j}(\omega_\mathrm{e}T_\mathrm{s})}\boldsymbol{v}_{\mathrm{dq}(0)}. \tag{31}$$

During T_s to $2T_\mathrm{s}$, the average voltage vector ($\boldsymbol{v}_{\mathrm{dq\_av}} = \boldsymbol{v}_{\mathrm{d\_av}} + \mathrm{j}\boldsymbol{v}_{\mathrm{q\_av}}$) can be used as the voltage vector acting in that time period. The average voltage vector $\boldsymbol{v}_{\mathrm{dq\_av}}$ can be derived as

$$\begin{aligned}\boldsymbol{v}_{\mathrm{dq\_av}} &= \frac{1}{T_\mathrm{s}}\int_{T_\mathrm{s}}^{2T_\mathrm{s}} \boldsymbol{v}_{\mathrm{dq}(T_\mathrm{s})}\cdot \mathrm{e}^{-\mathrm{j}\omega_\mathrm{e}(\tau-T_\mathrm{s})}\mathrm{d}\tau \\ &= \frac{2\sin(0.5\omega_\mathrm{e}T_\mathrm{s})}{\omega_\mathrm{e}T_\mathrm{s}}\mathrm{e}^{-\mathrm{j}(0.5\omega_\mathrm{e}T_\mathrm{s})}\boldsymbol{v}_{\mathrm{dq}(T_\mathrm{s})}.\end{aligned} \tag{32}$$

According to (31) and (32), the errors of d-axis and q-axis voltages caused by the delay of the controller can be expressed as

$$\begin{cases}\Delta v_\mathrm{d} = \left(\frac{1}{k}\cos(1.5\omega_\mathrm{e}T_\mathrm{s}) - 1\right)v_{\mathrm{d\_av}} - \frac{1}{k}\sin(1.5\omega_\mathrm{e}T_\mathrm{s})v_{\mathrm{q\_av}} \\ \Delta v_\mathrm{q} = \frac{1}{k}\sin(1.5\omega_\mathrm{e}T_\mathrm{s})v_{\mathrm{d\_av}} + \left(\frac{1}{k}\cos(1.5\omega_\mathrm{e}T_\mathrm{s}) - 1\right)v_{\mathrm{q\_av}}\end{cases} \tag{33}$$

$$k = \frac{2\sin(0.5\omega_\mathrm{e}T_\mathrm{s})}{\omega_\mathrm{e}T_\mathrm{s}} \tag{34}$$

where Δv_d and Δv_q are, respectively, the errors of d-axis and q-axis voltages between current controller output and the actual voltage applied to the motor.

When the motor works at the MTPA point, the voltage and current of the motor can be expressed as a function of torque. According to (30), (31), and the principle of MTPA control, the partial derivative error of the torque to d-axis and q-axis currents

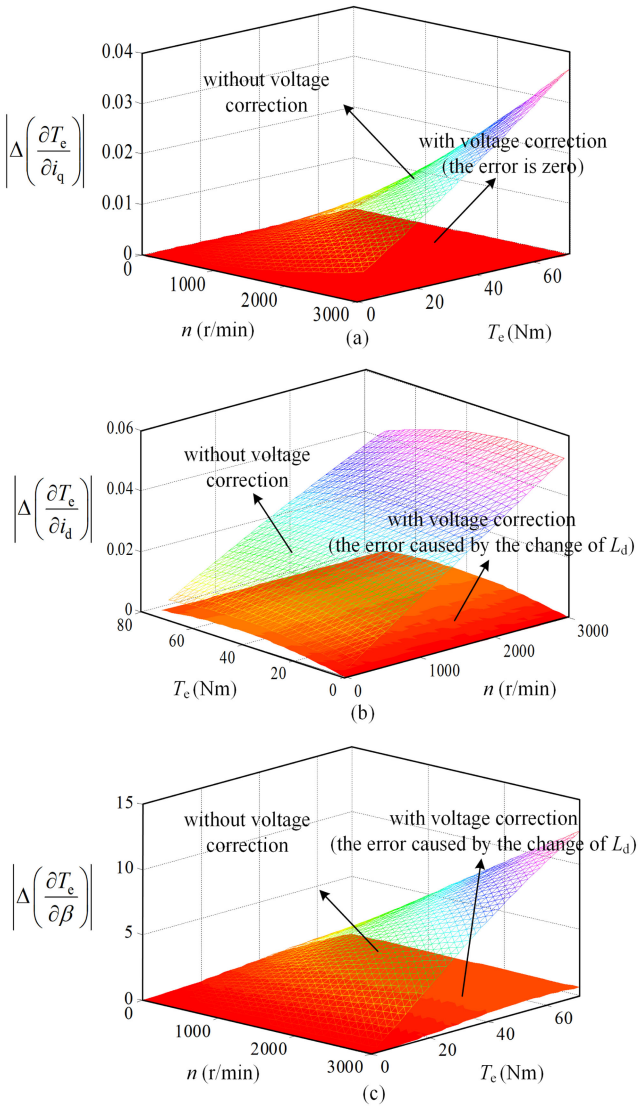

Fig. 6. Partial derivative error at different torque and speed. (a) Error of the partial derivative of torque to q-axis current. (b) Error of the partial derivative of torque to d-axis current. (c) Error of the partial derivative of torque to the current angle.

can be regarded as a function of the torque, speed, and control frequency

$$\begin{cases}\Delta\left(\frac{\partial T_\mathrm{e}}{\partial i_\mathrm{q}}\right) = f\left(\omega_\mathrm{e}, T_\mathrm{e}, T_\mathrm{s}\right) \\ \Delta\left(\frac{\partial T_\mathrm{e}}{\partial i_\mathrm{d}}\right) = f\left(\omega_\mathrm{e}, T_\mathrm{e}, T_\mathrm{s}\right) \\ \Delta\left(\frac{\partial T_\mathrm{e}}{\partial \beta}\right) = f\left(\omega_\mathrm{e}, T_\mathrm{e}, T_\mathrm{s}\right).\end{cases} \tag{35}$$

For the vehicle motor controller, a fixed control frequency is usually used. Fig. 6 shows the relation between the extracted partial derivative information error, motor torque, and speed when the motor works at MTPA point, and the control frequency is set to 10 kHz. It can be seen that the voltage error caused by the delay of the controller affects the extraction of partial derivative information. The error increases with the increase of torque and speed.

Therefore, in order to obtain accurate d-axis and q-axis voltages, it is necessary to correct the output voltage of the current controller. Combining (31) and (32), the scalar form of it can be expressed as

$$\begin{cases} v_{\mathrm{d\_av}} = k\left[v_{\mathrm{d0}}\cos(1.5\omega_{\mathrm{e}}T_{\mathrm{s}}) + v_{\mathrm{q0}}\sin(1.5\omega_{\mathrm{e}}T_{\mathrm{s}})\right] \\ v_{\mathrm{q\_av}} = k\left[v_{\mathrm{q0}}\cos(1.5\omega_{\mathrm{e}}T_{\mathrm{s}}) - v_{\mathrm{d0}}\sin(1.5\omega_{\mathrm{e}}T_{\mathrm{s}})\right]. \end{cases} \tag{36}$$

Equation (36) approximately describes the relation of the output of voltages output by the current controller and the voltages applied to the motor. By using voltage correction and dead-time compensation, relatively accurate motor terminal voltage information can be obtained.

Fig. 6 also shows the relation between the extracted partial derivative information error, motor torque, and speed after vlotage correction. It can be seen that the error of the partial derivative of the torque to the q-axis current is zero after the voltage correction. Due to the change of the d-axis inductance, the error of the partial derivative of the torque to the d-axis current still exists. However, it can be seen from the results that the error caused by the change of the d-axis inductance is much smaller than that caused by the rotor movement during one control period. At the same time, it also reflects that the change of d-axis inductance has little influence on the partial derivative information extraction.

C. Proposed Setting Method of d- and q-Axis Current References

1) Setting Method of d-Axis Current Reference: When the motor operates below the base speed, the extracted $\mathrm{d}T_{\mathrm{e}}/\mathrm{d}\beta$ is passed through the integrator to produce the d-axis current reference. With the action of the integrator, the d-axis current reference is gradually adjusted until $\mathrm{d}T_{\mathrm{e}}/\mathrm{d}\beta$ becomes zero, i.e., realizing the MTPA control. When the motor is operating in a flux weakening region, the difference between the output voltage vector amplitude of the current controller and the voltage limit is taken as feedback signal to correct the d-axis current reference.

2) Setting Method of q-axis Current Reference: In the field of electric vehicles, the control system expects the output torque to follow the given torque as much as possible. For this purpose, the reasonable setting of the q-axis current reference becomes the key to the torque output. When motor parameters are accurately obtained, the q-axis current reference can be set as [20]

$$i_{\mathrm{qref}} = T_{\mathrm{e\_ref}}/\frac{3}{2}n_{\mathrm{p}}\left[(L_{\mathrm{d}} - L_{\mathrm{q}})\, i_{\mathrm{dref}} + \lambda_{\mathrm{f}}\right]. \tag{37}$$

However, during the operation of the motor, its parameters are uncertain, and the q-axis current reference obtained from (37) cannot obtain the required torque. Considering that

$$\frac{\partial T_{\mathrm{e}}}{\partial i_{\mathrm{q}}} = \frac{3}{2}n_{\mathrm{p}}\left[(L_{\mathrm{d}} - L_{\mathrm{q}})\, i_{\mathrm{d}} + \lambda_{\mathrm{f}}\right]. \tag{38}$$

When the motor works in torque control mode, the d-axis current of the motor can follow the reference soon. So there is

$$i_{\mathrm{qref}} = T_{\mathrm{e\_ref}}/\frac{\partial T_{\mathrm{e}}}{\partial i_{\mathrm{q}}}. \tag{39}$$

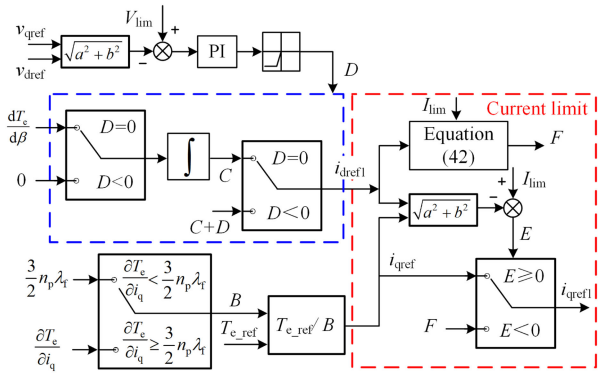

Fig. 7. Schematic of proposed d-axis and q-axis current reference generation.

Equation (39) cannot be used directly, it needs to make a modification as follows:

$$i_{\mathrm{qref}} = T_{\mathrm{e\_ref}}/B \tag{40}$$

$$B = \begin{cases} \frac{3}{2}n_{\mathrm{p}}\lambda_{\mathrm{f}}, & \frac{\partial T_{\mathrm{e}}}{\partial i_{\mathrm{q}}} < \frac{3}{2}n_{\mathrm{p}}\lambda_{\mathrm{f}} \\ \frac{\partial T_{\mathrm{e}}}{\partial i_{\mathrm{q}}}, & \frac{\partial T_{\mathrm{e}}}{\partial i_{\mathrm{q}}} \geq \frac{3}{2}n_{\mathrm{p}}\lambda_{\mathrm{f}}. \end{cases} \tag{41}$$

When the motor is started, $\partial T_{\mathrm{e}}/\partial i_{\mathrm{q}}$ changes from zero. In order to avoid the situation where the denominator is zero in (39), the initial value needs to be set. According to (38), when d-axis current is zero, $\partial T_{\mathrm{e}}/\partial i_{\mathrm{q}}$ is the smallest.

The q-axis current reference determined by the above equations can avoid the influence of motor parameters and realize the purpose of output torque following the given torque. Although i_{d} is not equal to i_{dref} in the transient process, the transient process itself is a regulation process. And the setting method proposed does not affect the implementation of the steady-state and dynamic process where i_{d} can follow i_{dref}. In the flux weakening region, when the amplitude of the given current vector is greater than the current limit with the increase of the motor speed, there should be the following constraints:

$$i_{\mathrm{qref1}} = \sqrt{I_{\mathrm{lim}}^2 - i_{\mathrm{dref}}^2}. \tag{42}$$

The block diagram of the proposed d-axis and q-axis current reference generation is shown in Fig. 7, and the control block diagram of the whole control system is shown in Fig. 8.

V. Experimental Results

To verify the feasibility of the theoretical analysis and the effectiveness of the proposed method, an experimental system, shown in Fig. 9, is set up. The experimental test bench consists of a dynamometer, a dc power supply, an inverter, and a control unit which is built by DSP(TMS320F28335) and FPGA(EP1C6Q240C8). Besides, an HBM-T12 torque sensor is used to measure the torque. The sampling frequency and carrier frequency of the control system are both 10 kHz. The parameters of the IPMSM are given in Table I.

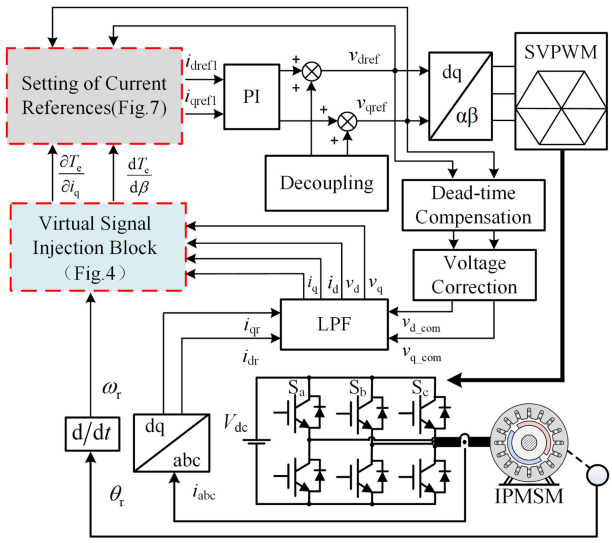

Fig. 8. Block diagram of the whole proposed control scheme.

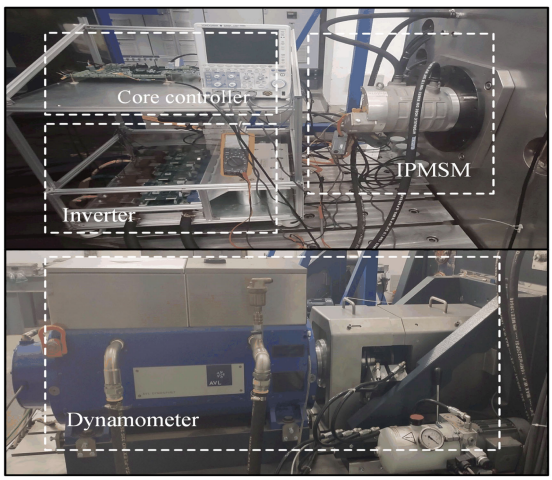

Fig. 9. Diagram of the experiment system.

TABLE I
PARAMETERS OF IPMSM

Paramerter	Symbol	Value	Unit
Pairs of poles	n_p	4	--
Permanent magnet flux	λ_f	0.073	Wb
Phase resistance	R	0.0034	Ω
d-axis inductance	L_d	0.146	mH
q-axis inductance	L_q	0.548	mH
Rated speed	n	3000	r/min
Rated torque	T_N	160	Nm
Rated voltage	U_N	320	V
Rated current	I_N	184	A
Curent limit	I_{lim}	260	A

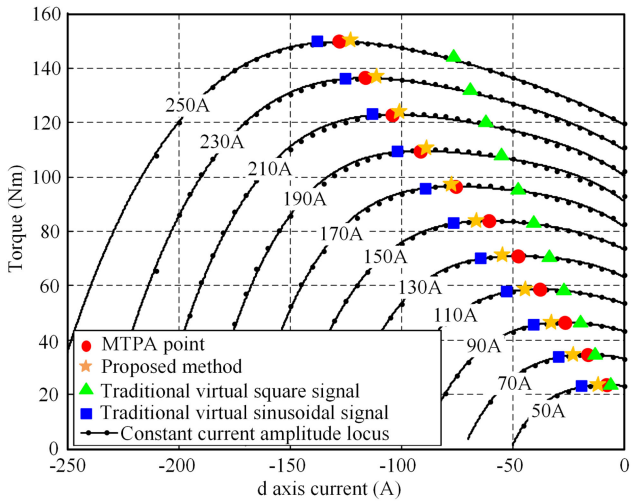

Fig. 10. MTPA tracking experimental results of traditional methods and proposed method at speed of 3000 r/min.

A. *Experimental Results Under the Base Speed*

Fig. 10 shows the experimental results of the MTPA tracking performance under the proposed method when the given current amplitude varies from 50 to 250 A in the step of 20 A at speed of 3000r/min. In order to verify the accuracy of the proposed method, the traditional virtual sinusoidal signal injection method and virtual square wave signal injection method are carried out as comparative experiments. As can be seen in Fig. 10, the d-axis reference obtained by the two traditional methods deviates from MTPA points. And the results obtained by the virtual square wave signal injection method deviates most seriously. It is obvious that the proposed method can track the MTPA points accurately.

In order to verify the influence of rotor position change caused by controller delay on the accuracy of MTPA point tracking, the virtual sinusoidal signal injection method and the virtual square wave signal injection method are modified with the voltages correction. The experimental results are shown in Fig. 11. Combining Figs. 10 and 11, it can be seen that the tracking accuracy of the traditional virtual sinusoidal signal injection method is improved with the additional voltage correction. And the results fit the experimental results of the proposed method well. However, the tracking accuracy of the virtual square wave signal injection method for MTPA point is still not good. The reason for that is the partial derivative information extracted is not accurate, which is caused by ignoring the higher order partial derivatives of torque with respect to β.

The accuracy of MTPA tracking affects the efficiency of IPMSM. In order to verify the advantages of the proposed method in the efficiency of the motor, virtual sinusoidal signal injection method, virtual square wave signal injection method, two traditional methods with voltage correction, and proposed method are used to observe the motor efficiency and output torque under different current amplitude references by Yokogawa-WT3000 power analyzer at 3000 r/min. The results

TABLE II
EFFICIENCY AND TORQUE COMPARISION OF SEVERAL CONTROL METHODS

I_s(A)	Virtual square signal injection method		Virtual sinusoidal signal injection method		Virtual square signal injection method with voltage correction		Virtual sinusoidal signal injection method with voltage correction		Proposed method	
	η(%)	T_e(Nm)	η(%)	T_e(Nm)	η(%)	T_e(Nm)	η(%)	T_e(Nm)	η(%)	T_e(Nm)
70	99.75	35.11	99.846	34.224	99.672	34.48	99.871	34.97	99.891	35.21
110	98.597	58.77	98.730	58.19	98.555	57.63	98.647	58.99	98.777	59.34
150	97.951	83.40	98.055	83.39	97.865	81.55	98.023	84.27	98.134	84.64
190	97.370	108.31	97.534	109.84	97.280	105.84	97.499	110.64	97.575	111.16
210	97.106	120.64	97.297	123.33	96.985	117.20	97.217	123.96	97.259	124.43
230	96.810	132.69	97.002	136.74	96.730	128.74	96.991	137.17	97.008	137.70
250	96.584	144.50	96.784	150.24	96.438	139.86	96.743	150.31	96.743	150.92

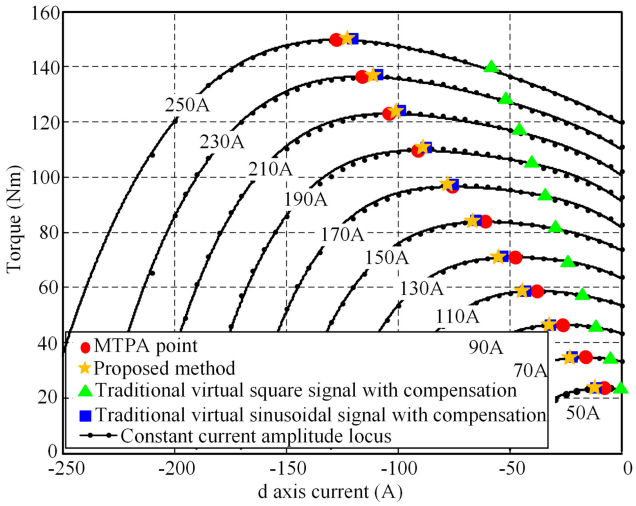

Fig. 11. MTPA tracking experimental results of traditional methods with voltage correction and proposed method at speed of 3000 r/min.

are illustrated in Table II. It can be seen that the efficiency and torque output of the two traditional methods are lower than that of the proposed method under the same current amplitude.

To further demonstrate the tracking performance for a torque reference, another experiment under 3000 r/min with a step change of torque reference from 10 to 160 Nm is carried out. Each process lasts for 2 s. The experimental waveforms of the proposed method and two traditional methods are shown in Figs. 12–14. Fig. 12(a) is the result of the traditional virtual sinusoidal signal injection method without voltage correction. As can be seen from it, the torque output is significantly less than the torque reference. The reason is that the q-axis current reference is obtained by the formula which is affected by the motor parameters. Fig. 12(b) is the result of this method with voltage correction. Torque output is still significantly less than the torque reference. Fig. 13 shows the results of the traditional virtual square signal injection method before and after voltage correction. It can be seen from Fig. 13(a) that the output torque obtained by this control method deviates from the torque reference, gradually. The reason is that it does not consider the voltage change caused by rotor position change, although this method achieves torque following through feedback control, which results in inaccurate feedback torque calculation. It can be seen from the waveform of Fig. 13(b) that the output torque of the motor can be close to the given torque with voltage correction. Fig. 14(a) shows the results of the proposed method without voltage correction. The output torque obtained by this control method also deviates from the torque reference, gradually. Fig. 14(b) is the result of the proposed method with voltage correction. It can be seen from the waveforms that the proposed method for setting the q-axis current reference can track the given torque better. By comparing the phase current waveforms in Fig. 13(b) and 14(b), it can be seen that under the same torque output, the current amplitude required by the traditional virtual square wave signal injection method is larger than the method proposed in this article. So, it is necessary to consider the voltage error caused by rotor position change for virtual signal injection methods. And the proposed method has better torque tracking performance than the traditional methods.

Fig. 15(a) and (b) shows the motor efficiency comparison between the virtual square wave signal injection method and the method proposed in this article when the output torque of the motor is 156 N·m and the speed is 3000r/min. It can be seen from the figures that the motor efficiency of the proposed method is 0.586% higher than that of the traditional virtual square wave signal injection method. Fig. 15(c) shows the motor efficiency comparison curves of the two methods under multiple output torques. It can be seen that the advantages of the proposed method become obvious with the increase of torque output.

The above experiments verify the superiority of the proposed method in MTPA control region. The experimental results of the proposed method in the flux weakening region are carried out in Section V-B.

B. Experimental Results in Flux Weakening Region

To verify the control effect of the proposed method in the flux weakening region, the proposed method is tested at a torque reference of 100 and 160 N·m, with the motor speed rising from 3000 to 7000 r/min at 200 r/min intervals. Moreover, comparison tests where q-axis current reference is calculated using the formula and the nominal parameters directly are carried

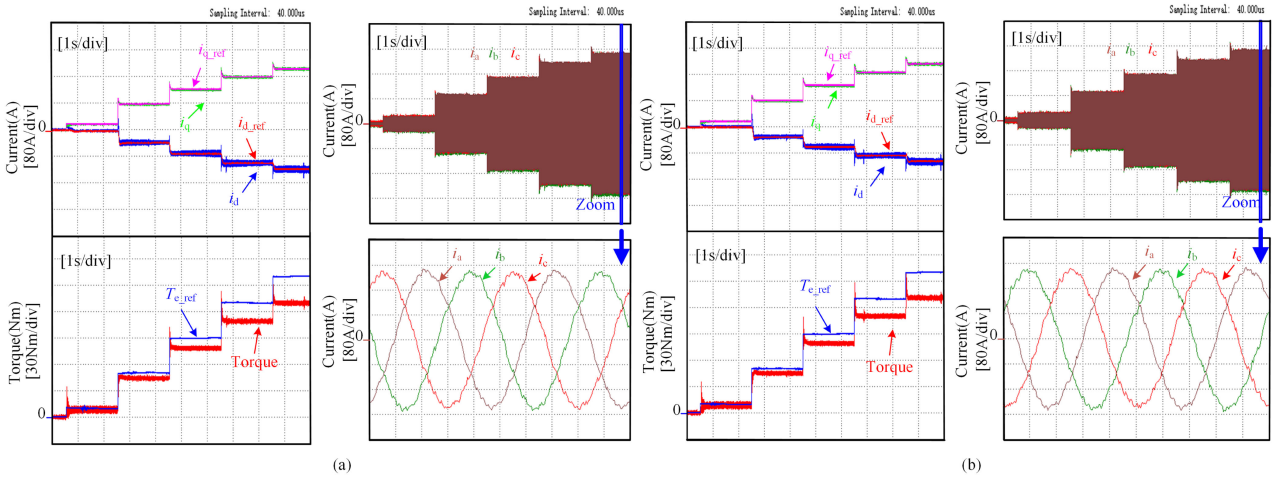

Fig. 12. Current and torque waveforms of the virtual sinusoidal signal injection method at speed of 3000 r/min and T_{e_ref} = 10, 50, 90, 130, 160 N·m. (a) Method without voltage correction. (b) Method with voltage correction.

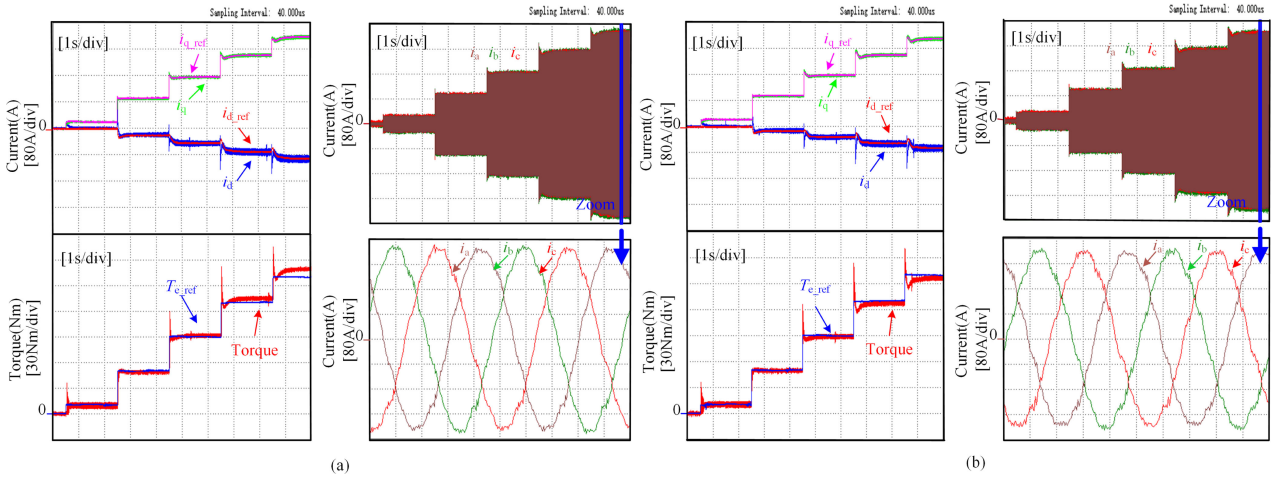

Fig. 13. Current and torque waveforms of the virtual square signal injection method at speed of 3000 r/min and T_{e_ref} = 10, 50, 90, 130, 160 N·m. (a) Method without voltage correction. (b) Method with voltage correction.

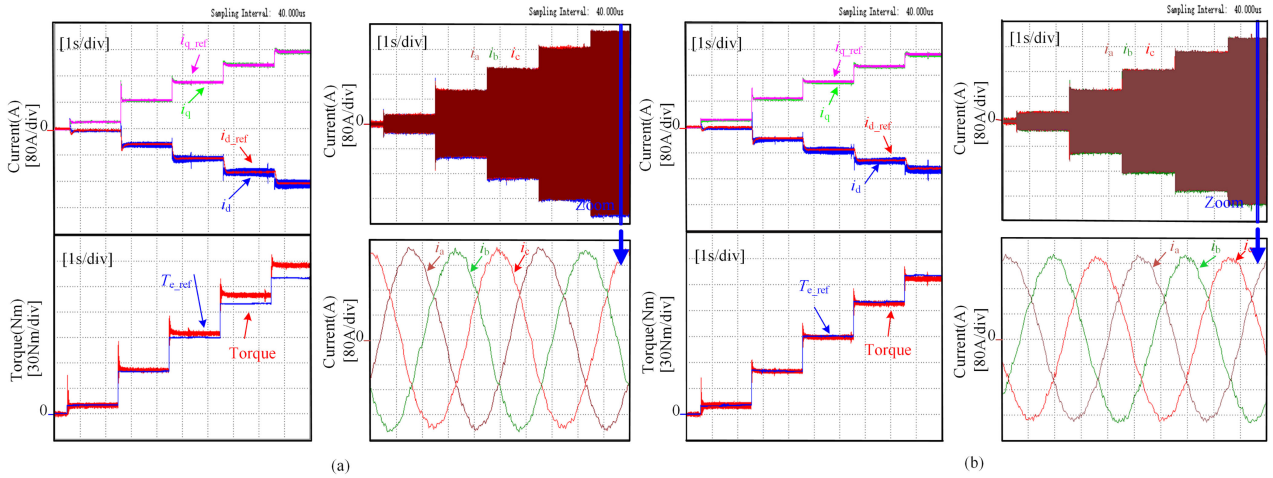

Fig. 14. Current and torque waveforms of proposed method at speed of 3000 r/min and T_{e_ref} = 10, 50, 90, 130, 160 N·m. (a) Method without voltage correction. (b) Method with voltage correction.

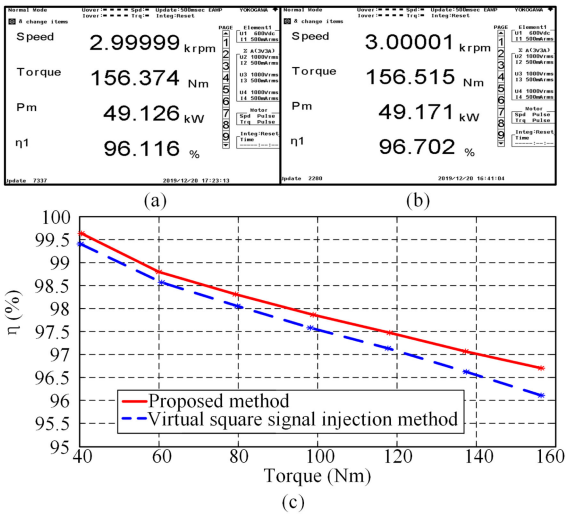

Fig. 15. Comparison diagram of motor efficiency with same motor torque output and speed. (a) Virtual square signal injection method. (b) Proposed method. (c) Motor efficiency comparison curves of the two methods under multiple output torques.

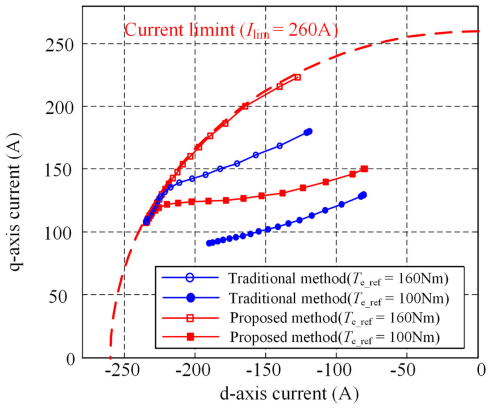

Fig. 16. d-axis and q-axis current tracks of two methods at speed of 3000–7000 r/min and T_{e_ref} = 100, 160 N·m.

out [23]. The d-axis current, q-axis current, and output torque of the motor of both methods are observed, respectively.

When the torque reference is 160 N·m and speed is 3000 r/min, it can be seen from Figs. 16 and 17 that the current amplitude of the proposed method is on the current limit circle, while that of the traditional method is in the current limit circle. The output torque of the motor under the traditional method is less than the torque reference, obviously. with the increase of speed, the current trajectory of the proposed method runs along the current limit circle, while the traditional method cannot guarantee the constant output torque before the current amplitude reaches the current limit circle because the setting of q-axis current reference depends on the motor parameters. When the torque reference is 100 N·m and speed is 3000 r/min, the current trajectory under the control of proposed method runs along the constant torque curve, first, and when the current amplitude reaches the current limit, the current trajectory runs along the current limit circle.

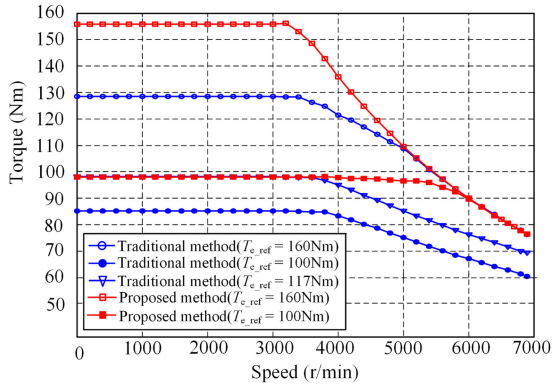

Fig. 17. Mechanical characteristic curve of two methods.

As can be seen, the output torque of the motor controlled by the traditional method deviates far from the torque reference. In order to compare the control effect of the motor with the same torque output, an experiment is carried out with a torque reference of 117 N·m under the traditional control method. As can be seen from Fig. 17, the method proposed has a wider range of constant torque region. And the output torque of the motor under the traditional control method is smaller than the output torque of the proposed method at 7000 r/min.

VI. Conclusion

In order to guarantee the speed range of constant torque region and improve the torque output capacity in FW region, the methods for determining the d-aixs and q-axis current references of IPMSM based on the existing virtual signal injection is researched in this article. A new strategy to extract $dT_e/d\beta$ is proposed based on the virtual constant signal which is superimposed on the d-axis and q-axis currents. And then, a scheme of d-axis and q-axis current references setting, which is applicable to constant torque region and FW region, is established by means of the partial derivative information. The advantages of the proposed method can be concluded as follows.

1) Filters that are essential in the virtual sinusoidal signal injection scheme are avoided. The acquisition of partial derivative information avoids the influence of neglecting high-order partial derivative term that the method of injecting virtual square wave signal along the current angle has.
2) The accuracy of derivative information that influences the current references is improved by considering the difference between the voltage output by the current controller and the actual voltage applied to the motor. So, the tracking of the MTPA point is more accurate than traditional methods.
3) The purpose of setting the q-axis current reference independent of the motor parameters is achieved by the partial derivative information of torque with respect to q-axis current. Thus, the speed range of the constant torque region is guaranteed.

REFERENCES

[1] S. Jung, J. Hong, and K. Nam, "Current minimizing torque control of the IPMSM using ferraris method," *IEEE Trans. Power Electron.*, vol. 28, no. 12, pp. 5603–5617, Dec. 2013.

[2] T. Shi, Y. Yan, Z. Zhou, M. Xiao, and C. Xia, "Linear quadratic regulator control for PMSM drive systems using nonlinear disturbance observer," *IEEE Trans. Power Electron.*, vol. 35, no. 5, pp. 5093–5101, May 2020.

[3] J. M. Kim and S. K. Sul, "Speed control of interior permanent magnet synchronous motor drive for the flux weakening operation," *IEEE Trans. Ind. Appl.*, vol. 33, no. 1, pp. 43–48, Jan./Feb. 1997.

[4] S. Morimoto, M. Sanada, and Y. Takeda, "Wide-speed operation of interior permanent magnet synchronous motors with high-performance current regulator," *IEEE Trans. Ind. Appl.*, vol. 30, no. 4, pp. 920–926, Jul./Aug. 1994.

[5] K. D. Hoang, J. Wang, and H. Aorith, "Online feedback-based field weakening control of interior permanent magnet brushless AC drives for traction applications accounting for nonlinear inverter characteristics," in *Proc. IET Int. Conf. Power Electron. Mach. Drives*, 2014, pp. 1–6.

[6] T. S. Kwon and S. K. Sul, "Novel antiwindup of a current regulator of a surface-mounted permanent-magnet motor for flux-weakening control," *IEEE Trans. Ind. Appl.*, vol. 42, no. 5, pp. 1293–1300, Sep./Oct. 2006.

[7] Y. C. Kwon, S. Kim, and S. K. Sul, "Voltage feedback current control scheme for improved transient performance of permanent magnet synchronous machine drives," *IEEE Trans. Ind. Electron.*, vol. 59, no. 9, pp. 3373–3382, Sep. 2012.

[8] S. J. Underwood and I. Husain, "Online parameter estimation and adaptive control of permanent-magnet synchronous machines," *IEEE Trans. Ind. Electron.*, vol. 57, no. 7, pp. 2435–2443, Jul. 2010.

[9] F. J. Lin, M. S. Huang, S. G. Chen, and C. W. Hsu, "Intelligent maximum torque per ampere tracking control of synchronous reluctance motor using recurrent legendre fuzzy neural network," *IEEE Trans. Power Electron.*, vol. 34, no. 12, pp. 12080–12094, Dec. 2019.

[10] K. Li and Y. Wang, "Maximum torque per ampere (MTPA) control for IPMSM drives based on a variable-equivalent-parameter MTPA control law," *IEEE Trans. Power Electron.*, vol. 34, no. 7, pp. 7092–7102, Jul. 2019.

[11] H. Wang, C. Li, G. Zhang, Q. Geng, and T. Shi, "Maximum torque per ampere (MTPA) control of IPMSM systems based on controller parameters self-modification," *IEEE Trans. Veh. Technol.*, vol. 69, no. 3, pp. 2613–2620, Mar. 2020.

[12] Z. Xia, S. Nalakath, R. Tarvidilu-Asl, Y. Sun, J. Wiseman, and A. Emadi, "Online optimal tracking method for interior permanent magnet machines with improved MTPA and MTPV in whole speed and torque ranges," *IEEE Trans. Power Electron.*, vol. 35, no. 9, pp. 9755–9771, Sep. 2020.

[13] R. Tarvidilu-Asl, S. Nalakath, Z. Xia, Y. Sun, J. Wiseman, and A. Emadi, "Improved online optimization-based optimal tracking control method for induction motor drives," *IEEE Trans. Power Electron.*, vol. 35, no. 10, PP. 10654–10672, Oct. 2020.

[14] S. Bolognani, R. Petrella, and A. Prearo, "Automatic tracking of MTPA trajectory in IPMmotor drives based on ac current injection," *IEEE Trans. Ind. Appl.*, vol. 47, no. 1, pp. 105–114, Jan. 2011.

[15] S. Kim, Y. Yoon, S. Sul, and K. Ide, "Maximum torque per ampere (MTPA) control of an IPM machine based on signal injection considering inductance saturation," *IEEE Trans. Power Electron.*, vol. 28, no. 1, pp. 488–497, Jan. 2013.

[16] G. Liu, J. Wang, and W. Zhao, "A novel MTPA control strategy for IPMSM drives by space vector signal injection," *IEEE Trans. Ind. Electron.*, vol. 64, no. 12, pp. 9243–9252, Dec. 2017.

[17] K. Li and Y. Wang, "Maximum torque per ampere (MTPA) control for IPMSM drives using signal injection and an MTPA control law," *IEEE Trans. Ind. Informat.*, vol. 15, no. 10, pp. 5588–5598, Oct. 2019.

[18] J. Xia, Y. Guo, Z. Li, J. Jatskevich, and X. Zhang, "Step-signal-injection-based robust MTPA operation strategy for interior permanent magnet synchronous machines," *IEEE Trans. Energy Convers.*, vol. 34, no. 4, pp. 2052–2061, Dec. 2019.

[19] X. Zhou, Y. Zhou, H. Wang, M. Liu, F. Zeng, and Y. Yu, "An improved MTPA control based on amplitude-adjustable square wave injection," *IEEE Trans. Energy Convers.*, vol. 35, no. 2, pp. 956–965, Jun. 2020.

[20] T. Sun, J. Wang, and X. Chen, "Maximum torque per ampere (MTPA) control for interior permanent magnet synchronous machine drives based on virtual signal injection," *IEEE Trans. Power Electron.*, vol. 30, no. 9, pp. 5036–5045, Sep. 2015.

[21] T. Sun, J. Wang, M. Koc, and X. Chen, "Self-learning MTPA control of interior permanent magnet synchronous machine drives based on virtual signal injection," *IEEE Trans. Ind. Appl.*, vol. 52, no. 4, pp. 3062–3070, Jul./Aug. 2016.

[22] T. Sun and J. Wang, "MTPA control of IPMSM drives based on virtual signal injection considering machines parameter variations," *IEEE Trans. Ind. Electron.*, vol. 65, no. 8, pp. 6089–6097, Aug. 2018.

[23] T. Sun and J. Wang, "Extension of virtual-signal-injection-based MTPA control for interior permanent-magnet synchronous machine drives into the field-weakening region," *IEEE Trans. Ind. Electron.*, vol. 62, no. 11, pp. 6809–6817, Nov. 2015.

[24] T. Sun and J. Wang, "On accuracy of virtual signal injection based MTPA operation of interior permanent-magnet synchronous machine drives," *IEEE Trans. Power Electron.*, vol. 32, no. 9, pp. 7405–7408, Sep. 2017.

[25] Q. Tang, A. Shen, P. Luo, W. Li, and X. He, "IPMSMs sensorless MTPA control based on virtual q-axis inductance by using virtual high frequency signal injection," *IEEE Trans. Ind. Electron.*, vol. 67, no. 1, pp. 136–146, Jan. 2020.

[26] J. Wang and X. Huang, "An accurate virtual signal injection control of MTPA for an IPMSM with fast dynamic response," *IEEE Trans. Power Electron.*, vol. 33, no. 9, pp. 7916–7926, Sep. 2018.

[27] M. Li, S. Huang, X. Wu, K. Liu, X. Peng, and G. Liang, "A virtual HF signal injection based maximum efficiency per ampere tracking control for IPMSM drive," *IEEE Trans. Power Electron.*, vol. 35, no. 6, pp. 6102–6113, Jun. 2020.

[28] Y. C. Kwon, S. K., and S. K. Sul, "Six-step operation of PMSM with instantaneous current control," *IEEE Trans. Ind. Appl.*, vol. 50, no. 4, pp. 2614–2625, Jul./Aug. 2014.

[29] T. S. Kwon, G. Y. Choi, M. S. Kwak, and S. K. Sul, "Novel flux weakening control of an ipmsm for quasi-six-step operation," *IEEE Trans. Ind. Appl.*, vol. 44, no. 6, pp. 1722–1731, Nov./Dec. 2008.

[30] P. Y. Lin and Y. S. Lai, "Voltage control technique for the extension of dc-link voltage utilization of finite-speed spmsm drives," *IEEE Trans. Ind. Electron.*, vol. 59, no. 9, pp. 3392–3402, Sep. 2012.

[31] B. H. Bea, N. Patel, S. Schulz, and S. K. Sul, "New field weakening technique for high saliency interior permanent magnet motor," in *Proc. Conf. Rec. IEEE IAS Annu. Meet.*, 2003, pp. 898–905.

[32] Y. Z. Chen, X. Y. Huang, and J. Wang, "Improved flux-weakening control of IPMSMs based on torque feedforward technique," *IEEE Trans. Power Electron.*, vol. 33, no. 12, pp. 10970–10978, Dec. 2018.

[33] B. Cheng and T. R. Tesch, "Torque feedforward control technique for permanent-magnet synchronous motors," *IEEE Trans. Ind. Electron.*, vol. 57, no. 3, pp. 969–974, Mar. 2010.

[34] B. H. Bae and S. K. Sul, "A compensation method for time delay of full-digital synchronous frame current regulator of PWM AC drives," *IEEE Trans. Ind. Appl.*, vol. 39, no. 3, pp. 802–810, Mar./Jun. 2003.

Zhiwei Chen was born in Pingdingshan, China, in 1994. He received the B.S.degree in electrical engineering from China University of Mining and Technology, Xuzhou, China, in 2017. He is currently working toward the Ph.D. degree in electrical engineering with the School of Electrical and Information Engineering, Tianjin University, Tianjin, China.

His research interests include electrical machines, motor drives, and power electronics.

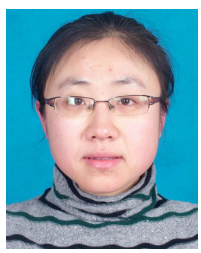

Yan Yan was born in Tianjin, China, in 1981. She received the B.S. and M.S. degrees from the Tianjin University of Science and Technology, Tianjin, China, in 2004 and 2007, respectively, and the Ph.D. degree from Tianjin University, Tianjin, China, in 2010, all in electrical engineering.

She is currently an Associate Professor with the College of Electrical Engineering, Zhejiang University, Hangzhou, China. Her current research interests include electrical machines and their control systems, power electronics, and electric drives.

Tingna Shi (Member, IEEE) was born in Yuyao, China, in 1969. She received the B.S. and M.S. degrees from Zhejiang University, Hangzhou, China, in 1991 and 1996, respectively, and the Ph.D. degree from Tianjin University, China, in 2009, all in electrical engineering.

She is currently a Professor with the College of Electrical Engineering, Zhejiang University, Hangzhou, China. Her current research interests include electrical machines and their control systems, power electronics, and electric drives.

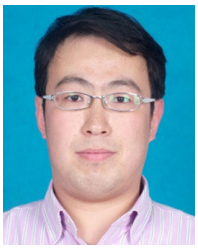

Xin Gu (Member, IEEE) was born in Tianjin, China, in 1980. He received the B.S., M.S., and Ph.D. degrees from Tianjin University, Tianjin, China, in 2003, 2006 and 2010, all in electrical engineering.

He joined Tiangong University, as a Lecturer, in 2010. He is currently an Associate Professor with the College of Electrical Engineering and Automation, and also with the National Local Joint Engineering Research Center of Electric Machine System Design and Manufacturing, China. His research interests include permanent magnet synchronous machines and their control systems.

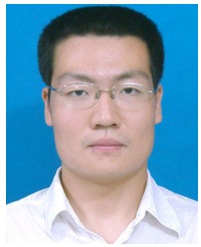

Zhiqiang Wang (Member, IEEE) was born in Tianjin, China, in 1984. He received the B.S. degree from the Hebei University of Technology, China, in 2002, and the M.S. and Ph.D. degrees from Tianjin University, China, in 2008 and 2012, respectively, all in electrical engineering.

He is currently an Associate Professor with the School of Artificial Intelligence, Tiangong University, China. His research interests include power electronics technology and intelligent control of motor systems.

Changliang Xia (Senior Member, IEEE) was born in Tianjin, China, in 1968. He received the B.S. degree from Tianjin University, China, in 1990, and the M.S. and Ph.D. degrees from Zhejiang University, China, in 1993 and 1995, respectively, all in electrical engineering.

He was a Full Professor with the School of Electrical Engineering and Automation, Tianjin University, Tianjin, China, in 2002. Since 2018, he has been the President of Tiangong University, Tianjin, China, where he is currently a Full Professor and the Director of the National Local Joint Engineering Research Center of Electrical System Design and Manufacturing. He also serves as the Qiushi Chair Professor of Zhejiang University, Hangzhou, China. He has published more than 200 journal papers, four books, and 60 patents. His fields of research interests include electrical machines, power electronics, and their control systems.

Dr. Xia was elected as an Academician of the Chinese Academy of Engineering in 2017. He has won the State Science and Technology Award of China twice.